Velocity estimation by the CRS method: A GPR real data example

Hervé Perroud (IGP, University of Pau, Av. de l'Université, 64013 Pau Cedex, France) and
Martin Tygel (LGC, State University of Campinas, CP 6065, CEP 13081-970, Campinas, Brazil)

This paper was prepared for presentation at the 8th International Congress of The Brazilian Geophysical Society held in Rio de Janeiro, Brazil, 14-18 September 2003.

Abstract

We describe the use of the Common Reflection Surface (CRS) method to estimate velocities from Ground Penetrating Radar (GPR) data. Applied to GPR multi-coverage data, the CRS method provides, as one of its outputs, the time-domain rms-velocity map that is then converted to depth by the familiar Dix algorithm. Combination of the obtained depth-converted velocity map with in situ measurements of electrical resistivity enables to estimate both water content and water conductivity. These quantities are essential to delineate infiltration of contaminants from the surface after industrial or agriculture activities. The method has been applied to a real dataset and compared with the classical NMO approach. The results show that the CRS method provides a much more detailed velocity field, thus improving the potential of GPR as an investigation tool for environmental studies.

INTRODUCTION

The CRS method is a novel seismic time-imaging technique (Hubral, 1999) that provides also attributes related to the subsurface model. These attributes, expressed in terms of wavefront curvatures and emergence angle, can be combined to estimate the RMS velocities within the illuminated part of the subsurface model. The purpose of this paper is to investigate the ability of the CRS method to retrieve RMS velocities (together with their corresponding interval velocities), as compared with the classical normal moveout (NMO) approach. For the comparison, we use a real dataset obtained from a near-surface GPR multi-offset survey. In this way, the ability of the CRS method to handle the specificities of electro-magnetic waves, such as unusual scaling and medium attenuation, can be assessed. Furthermore, the interval velocities, obtained after conversion of the GPR velocities, are combined with parallel electrical resistivity measurements to recover groundwater properties such as water content or water conductivity. This combination allows for a better understanding of the physical meaning of the original GPR velocities, as obtained by classical NMO and the CRS procedures. Finally, as the GPR experiments were repeated in time, we were able to monitor the stability of these velocity determinations.

There are three main factors that contribute to the bulk conductivity in a porous soil, namely the water content, the water conductivity, and the clay content, provided that the matrix can be considered as insulating. For environmental issues such as the monitoring of contaminant infiltration, one important objective is to evaluate the water conductivity, mainly in the vadose zone between the surface and the aquifer nappe, where the water content is highly variable. As a consequence, we need independent measurements, so as to separate the effect of these parameters. Following the strategy proposed in Garambois et al. (2002), we use, as a first step, GPR velocity to estimate water content. As a next step, we combine the obtained results with the electrical resistivity measurements to delineate water-conductivity anomalies. The anomalies that remain stationary in time will be attributed to clay, while the ones that vary with time will be interpreted as an evidence for the diffusion of a solution in the ground water. It is thus of primary importance to get the most detailed and reliable GPR velocity field estimation. To make it feasible in an industrial context, the whole procedure is required to be easily implemented and processed. This means that the experimental setup should be simple and the data processing should be as most automatic as possible.

THE GPR DATASET

Multi-coverage GPR dataset is not common, since most acquisition systems have only one channel. GPR investigation is therefore usually conducted in a single common-offset configuration. In the same way as in seismics, the GPR method provides a time image of the subsurface (electromagnetic) reflectors and diffractors. For migration or depth conversion purposes, a few CMP experiments are, in general, also made, the obtained velocities being interpolated between them. Due to a new generation of multi-channel instruments, GPR investigation practices are changing to use their improved capabilities. In this study, GPR data acquisition was conducted with a Ramac-2 4 channels control unit manufactured by Mala Geophysics, together with 2 pairs of unshielded 200 Mhz antennas. The multi-offset coverage data were obtained by repeated pro-

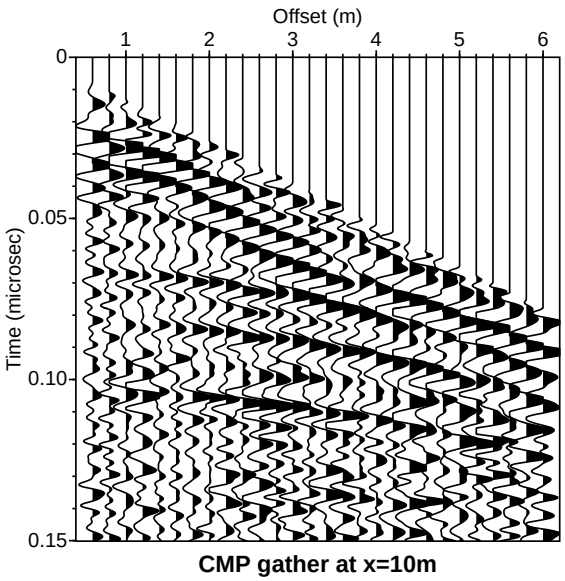

Figure 1: Example common mid-point gather for position x=10m

filing with the 4 antennas mounted on a PVC cart with varying spacings. Altogether, we obtained 28 different offsets, every 0.2 m from 0.6 to 6 m, for each CMP spaced every 0.1 m on a 55 m long profile. The traces were sampled over 0.15 microseconds, what corresponds roughly to a 6 m penetration depth for a mean velocity of $0.75\,10^8$ m/s. These procedures were repeated over time to monitor the changes in the subsurface water properties. In this on-going project, we achieved a full-year coverage at one-month time intervals.

Standard processing was applied to the datasets, including static shift for zero time, mean amplitude removal, tapered bandpass filtering and mute of air wave. Moreover, amplitude balancing were achieved through a division of each common-offset gather by the mean of its envelope traces. The final datasets were then sorted into CMP gathers for velocity estimation and stacking. A typical common midpoint (CMP) gather is shown in Figure 1. It reveals a series of coherent hyperbolic reflection-time curves that should allow a precise determination of the GPR velocity field. Some artifacts (ringing) due to the interaction between antennas in our multi-offset configuration appear uncorrelated from trace to trace. On the same profile, an electrical resistivity section was obtained with a 64-electrode Syscal-R2 system from Iris Instruments, with electrode interval of 1 m. Measured apparent resistivities were converted into a 2D resistivity section using the inversion algorithm of Loke and Barker (1996), with random residuals less than few percents. The obtained resistivity section, shown in Figure 4, reveals both vertical and lateral variations. As shown below, these provide interesting comparisons with our GPR velocity estimations.

VELOCITY MODEL ESTIMATION

RMS velocity estimation with classical NMO

The procedure followed here to derive the velocity field involves, in a first step, a classical NMO-velocity analysis, performed with the aid of the SU seismic processing software. Semblance maps were computed for a selection of CMPs, spaced every 2m along the whole profile. For these, semblance maxima were manually picked for each reflection-time curve. In a second step, to overcome the inaccuracy of the picking due to the elongation of the semblance maxima along the velocity axis, the previously obtained velocities were refined by means of visual adjustment of the corresponding hyperbolae on the CMP data. This is possible only when the signal-to-noise ratio of the analyzed event is significantly higher than 1, what is not achieved everywhere in the section. From the set of obtained time-velocity laws spaced along the profile, a bilinear interpolation was applied to generate a complete velocity map, namely one that is defined for all time samples and all midpoints. The obtained RMS velocity field is shown in Figure 2.

RMS velocity estimation with the CRS method

The procedure to derive the velocity field from the CRS method comprises 3 steps. First the CRS software (version 4.2, University of Karlsruhe (Mann, 2002)) was used to obtain the optimized CRS attributes for all samples and all CMPs, after adjustement of critical parameters like the apertures which define the size of the CRS super-gathers. Second, the RMS velocities were computed from these attributes, and cleaned according to chosen thresholds regarding the coherency estimation and number of traces used, what leads to the Vrms velocity field shown in Fig. 2. Third, the obtained velocity field was interpolated to fill the gaps, exprapolated to the limit of the studied domain and smoothed. The obtained RMS velocity field is shown in Figure 3.

NMO-CRS comparison

Figures 2 and 4 are directly comparable, since they represent the same information, at the same level of the processing. It can be observed that the values are in general agreement, as well as the overall organization, namely as a three layer model. However, thanks to the (automatic) computation of the stacking velocity at all time samples and CMPs, the CRS section presents much more detailed variations of the velocity field (Figure 3) than its counterpart, classical NMO section. As a consequence, it is expected that, with the help of the CRS method, more useful geophysical infor-

mation could be recovered (e.g., after inversion to interval velocities).

Interval velocity fields

The interval velocity derived from their corresponding RMS-velocity sections obtained by classical NMO and CRS are shown in Figures 6 and 7, and compared to the electrical section (Figure 5). Except for a few values which exceed the shown velocity range (the slight anomalies, in yellow-red, with velocities lower than 5000 cm/microsec that can be considered as improbable), both sections present acceptable velocity values, and a reasonable general three-layered organization. Most of both sections present middle to high velocity values that are physically meaningful, given the known soil context. Note that the most unrealistic values from the CRS section are restricted to its lower right part, which is not well constrained by the available data.

The vertical and lateral consistency of the velocity fluctuations seem much better in the CRS section, especially in the left part where the velocity estimations are most abundant and well determined. Furthermore, the overall velocity distribution of this same section relates much better to the corresponding independent electrical resistivity section. Both sections present anomalies in the same depth range and with local extrema in the same midpoint position (10m, 33m, 51m). The same good qualities cannot be found in the classical NMO velocity section. It seems, therefore, that the CRS section can be much more easily correlated with other available geophysical evidences. That is precisely what we need for the present objective to groundwater characterizations.

Time monitoring

As a last test to evaluate the physical meaning of CRS-recovered velocity estimations, we processed with exactly the same CRS parameters three datasets from the same site, obtained at three different times, and corresponding to different moisture conditions. The water level was also monitored, in a well just adjacent to the profile. The already processed dataset corresponds to intermediate water-content, with a water table at 240 cm depth. We selected for comparison a dataset for a high water content, with a water table at 180 cm depth (called wet condition), and one with low water content, with water table at 303 cm depth (called dry condition). The comparison was made on interval velocities in depth, rather than RMS velocities in time, to allow an easier check with the water-table levels. The CRS provides automatically interval velocity fields for these three datasets that are quite consistent, with similar patterns but significant differences.

As theoretically expected, we can observe in Figure 8 that the CRS interval velocities are linked to the moisture conditions. They appear to increase when the water content diminishes, as a result of the deepening of the water table. Furthermore, the velocity changes are concentrated in the part of the sub-surface where the water table and thus the water content vary. We are therefore quite confident that the CRS velocity determinations have given us physically meaningful estimations of the GPR velocity. These are needed to assess first the water content, and then, after combining it with the electrical measurements, the fluid conductivity.

CONCLUSIONS

By means of a GPR real data example, we have examined the ability of the CRS method to estimate rms-velocities that can be further inverted to a meaningful interval velocity field. The comparison between the velocity analyses conducted, on the one hand by means of the classical NMO method, and on the other hand by means of the CRS method, demonstrates that the latter delivers a clearer and more detailed rms-velocity field than the former in most parts of the section. The inverted interval velocity field obtained by the CRS method looks in most parts physically more consistent than the corresponding one inverted using classical NMO. The correlation of anomalies in the CRS interval velocity field and the electrical resistivity section confirms this fact. It also follows the water-content variation with time. Therefore, the CRS velocity field, in combination with electrical measurements, seems to be more suitable for the evaluation of ground-water properties than the classical NMO velocity field.

ACKNOWLEDGEMENTS

We thank the Research Foundation of the State of São Paulo (FAPESP - Brazil, grants 01/01068-0, 02/06590-0) for its financial support and H. Perroud's stay at the Applied Mathematics Department, University of Campinas, Brazil. The GPR data were acquired and processed with the help of P. Senechal, and financed by a grant from the French ACI Eau-Environnement program.

References

Garambois, S., Sénéchal, P., and Perroud, H., 2002, On the use of combined geophysical methods to assess water content and water conductivity of near-surface formations: J. of Hydrology, **259**, 32–48.

Hubral, P., Ed., 1999, Macro-model independent seismic reflection imaging, volume 42, 3-4 J. Appl. Geophys.

Loke, M., and Barker, R., 1996, Rapid least-squares inversion of apparent resistivity pseudosections using a quasi-newton method: Geophys. Prospect., **44**, 131–152.

Mann, J., 2002, Extensions and applications of the common-reflection-surface stack method: Logos Verlag, Berlin.

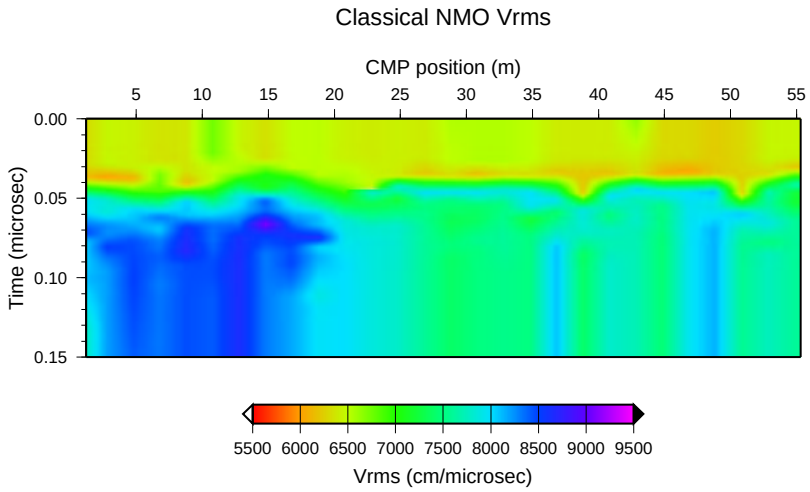

Figure 2:

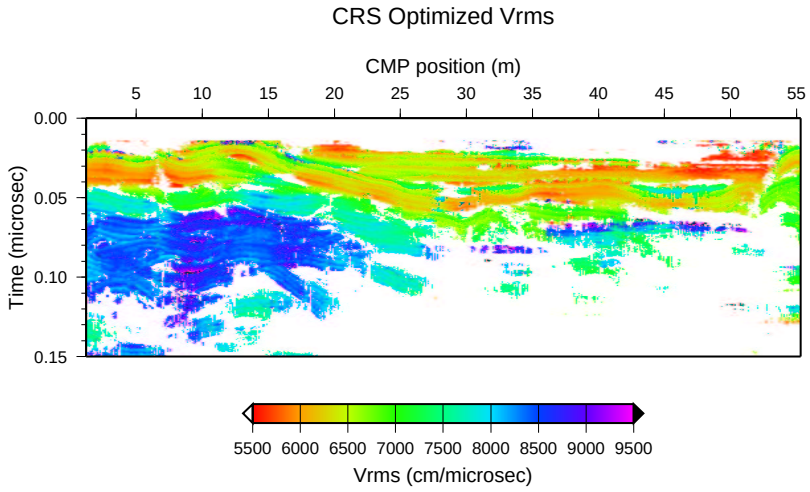

Figure 3:

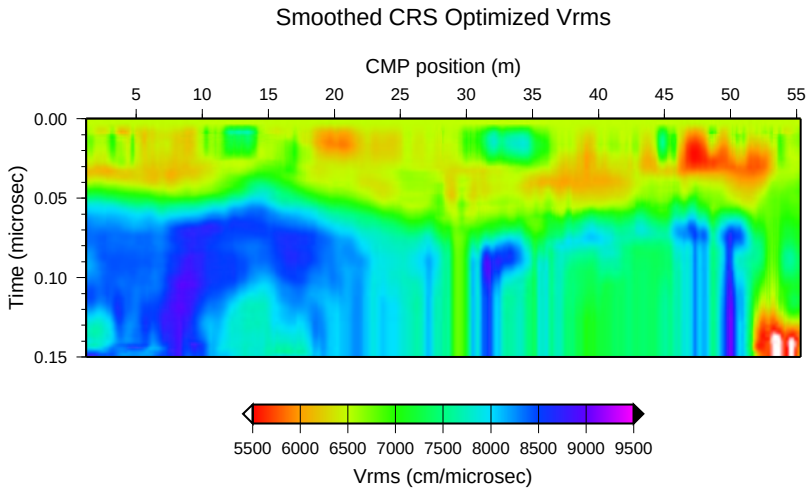

Figure 4:

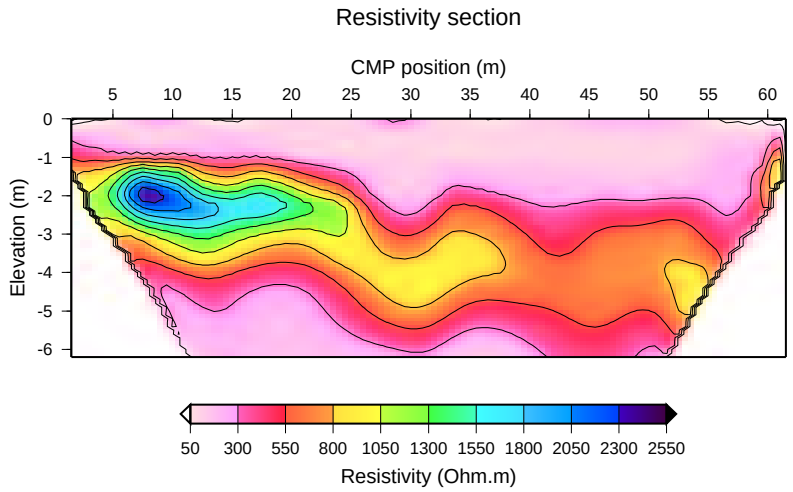

Figure 5:

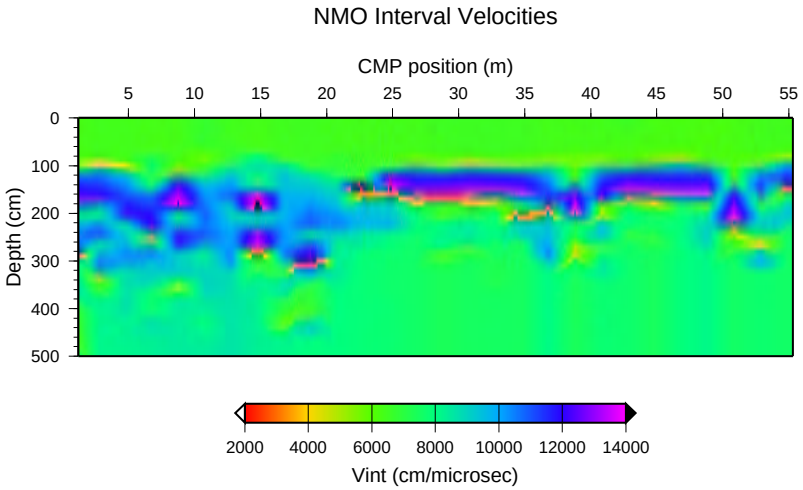

Figure 6:

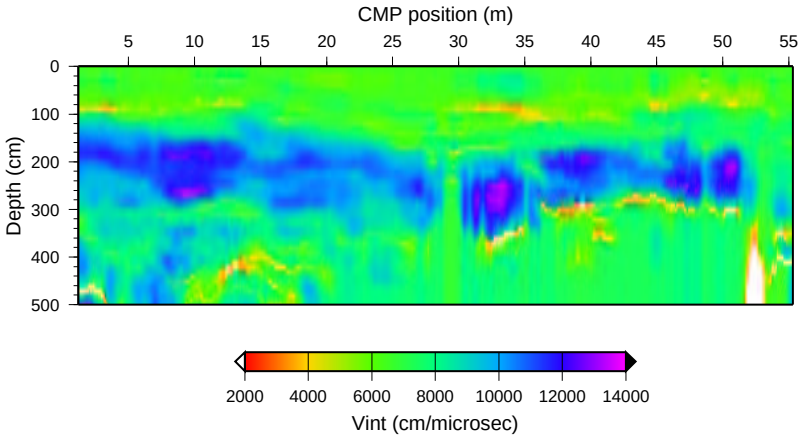

Figure 7:

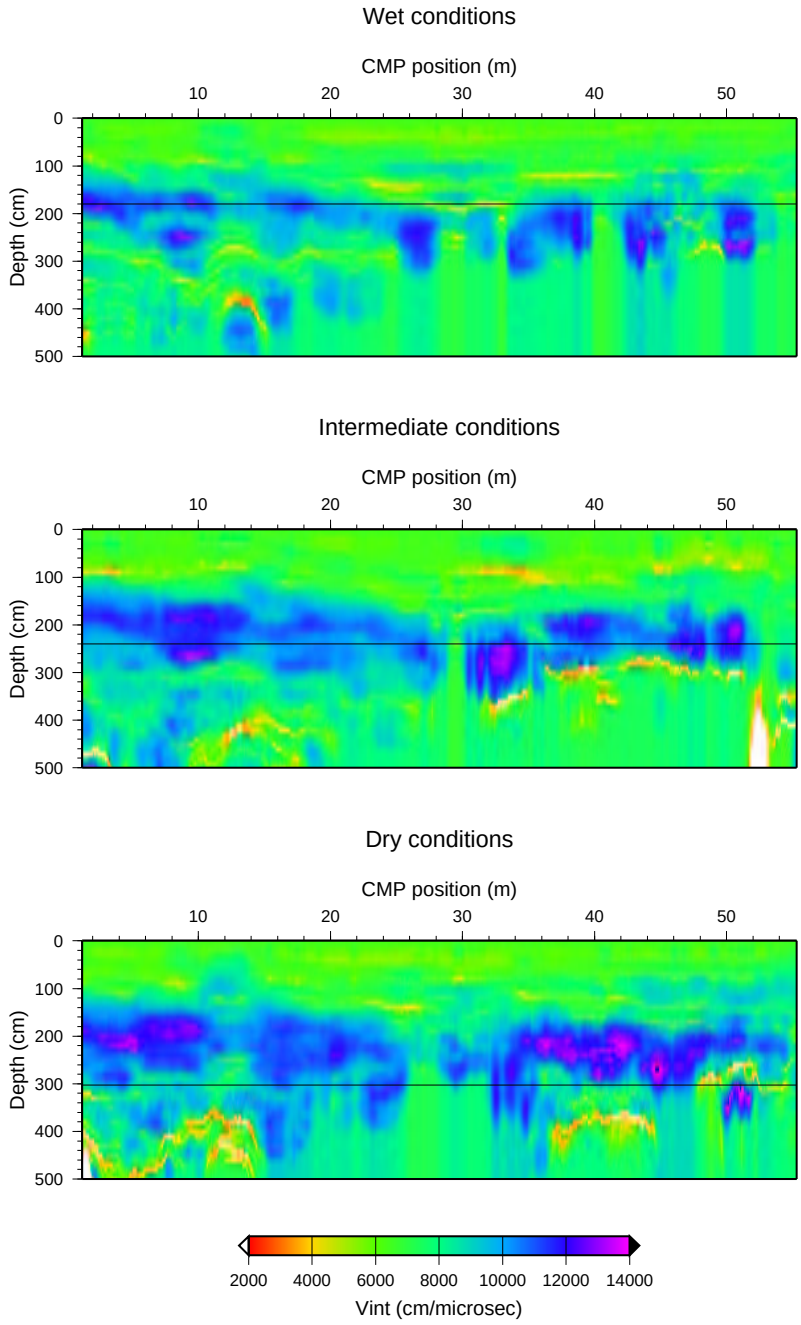

Figure 8: CRS-derived interval velocity maps for three different periods, with varying moisture conditions. The water level, as measured in a neighbouring well, is shown as the horizontal black line.